Half-meter Scale Superconducting Magnetic Bearing for Cosmic Microwave Background Polarization Experiments

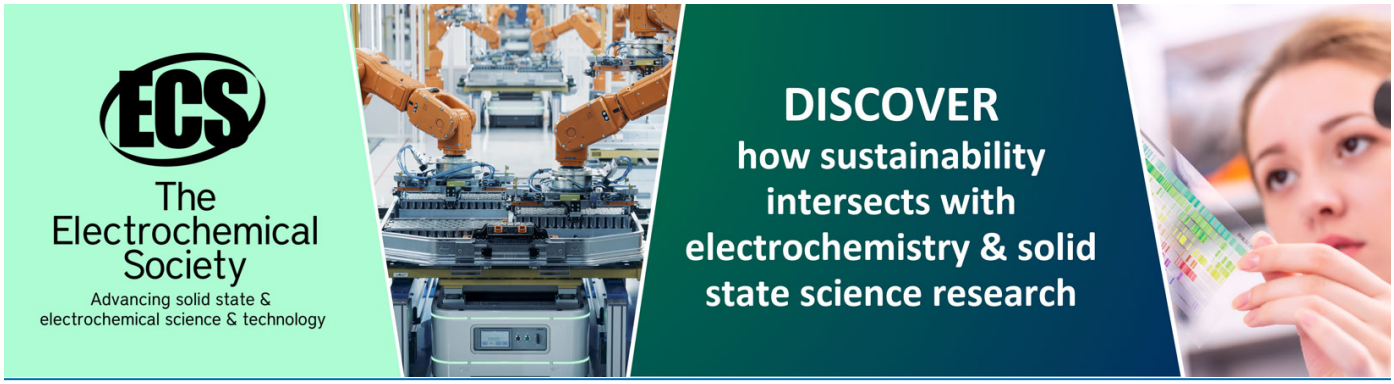

Half-meter Scale Superconducting Magnetic Bearing for Cosmic Microwave Background Polarization Experiments

Yuki Sakurai[1], Peter Ashton[2,3,1], Akito Kusaka[3,4,5,6], Charles A. Hill[2,3], Kenji Kiuchi[4], Nobuhiko Katayama[1], Osamu Tajima[7]

[1] Kavli Institute for The Physics and Mathematics of The Universe (WPI), The University of Tokyo, Kashiwa, Chiba 277-8583, Japan
[2] Department of Physics, University of California, Berkeley, CA 94720, USA,
[3] Physics Division, Lawrence Berkeley National Laboratory, Berkeley, CA 94720, USA
[4] Department of Physics, The University of Tokyo, Tokyo 113-8654, Japan,
[5] Kavli Institute for the Physics and Mathematics of the Universe (WPI), Berkeley Satellite, the University of California, Berkeley 94720, USA
[6] Research Center for the Early Universe, School of Science, The University of Tokyo, Tokyo 113-0033, Japan
[7] Department of Physics, Kyoto University, Kyoto 606-8502, Japan
E-mail: yuki.sakurai@ipmu.jp

Abstract We report the development of a large-diameter superconducting magnetic bearing (SMB) used in a continuously rotating cryogenic half-wave plate (HWP) polarization modulator for cosmic microwave background (CMB) polarization experiments. A precise measurement of the CMB polarization will place tighter constrains on cosmic inflation, describing the rapid expansion of the early universe. The polarization modulator is a critical instrument for suppressing 1/f contamination, which is mainly caused by atmospheric noise, and for mitigating systematic uncertainties that arise when differencing orthogonal polarization detectors. To ensure a sufficient field of view and to reduce thermal emission, the polarization modulator must have a clear-aperture diameter of > 500 mm and must operate at cryogenic temperatures. We constructed a superconducting magnetic bearing (SMB) with an inner diameter of 550 mm, which is the largest used in any CMB polarization experiment to date. We tested the friction and stiffness of the bearing at liquid nitrogen temperatures. The measured total loss is 0.4 W and the spring constant is $>10^5$ N/m, which satisfies typical experimental requirements. Furthermore, we performed a performance test by changing the number of disk-shaped YBCO tiles, and then confirmed that the SMB performance was proportional to the YBCO volume.

1. Introduction

Superconducting technologies are not only applied to industrial applications but also to fundamental physics experiments in various observation instruments, such as detectors and accelerators. In this paper, we describe a unique applications of the magnetic levitation technique: a superconducting magnetic bearing (SMB) for polarization modulators used in cosmic microwave background (CMB) polarization experiments.

The CMB is electromagnetic radiation from the Big Bang, the oldest light in the universe, which we can observe isotropically in whole sky even today. Moreover, CMB observation satellites can detect CMB intensity precisely, and their data have played a significant role in the formation of current cosmology. However, mysteries such as the flatness and horizon problems still exist in modern cosmology. As the cosmic inflation theory [1,2] is considered to solve these problems, the experimental verification of inflation is one of the most important research topics in both cosmology and high-energy physics. Cosmic inflation is the rapid expansion of the universe $\sim 10^{-38}$ seconds after the beginning of the universe. It is predicted that primordial gravitational waves are generated during inflation, and a characteristic "B-mode" pattern is imprinted in the CMB polarization by these primordial gravitational waves. Therefore, the inflation theory can be verified experimentally by a precise measurement of the B-mode polarization.

In a CMB polarization experiment, a key instrument is the polarization modulator based on the continuously rotating half-wave plate (HWP), an optical element that causes a half-wave phase shift of an linearly polarized incident signal [3]. It consists of the HWP and a rotation mechanism and modulates the CMB polarization signal. This modulation suppresses 1/f contamination mainly caused by atmospheric noise and mitigates the systematic uncertainties that arise when differencing between orthogonal polarization detectors. In order to suppress thermal noise, the HWP must be installed in a cryogenic environment. Thus, it is crucial to develop a completely contactless rotation mechanism (a bearing and drive motor) to achieve a stable rotation at low temperatures. A superconducting magnetic bearing (SMB) [4] is most suitable for this application. The polarization modulator using an SMB had been previously installed in a balloon experiment EBEX [5], and its benefits have been illuminated. As such, an on-going ground experiment, Simons Array [6], and a next-generation ground experiment, Simons Observatory (SO) [7], have employed the SMB in their polarization modulators.

One of the fundamental challenges in using the SMB in future experiments --represented by SO in this paper-- is the diameter limitation. To ensure a sufficient field of view, the SMB must have a clear-aperture diameter of > 500 mm. Therefore, we constructed an SMB with an inner diameter of 550 mm, which is the largest used in any CMB polarization experiment to date. In this paper, we describe the design of the developed SMB with the largest diameter for polarization modulators and its mechanical and thermal characteristics from liquid-nitrogen testing.

2. SMB and experimental setup

2.1. SMB design and manufacturing

The representative requirements for the polarization modulator in ground experiments, which are derived from science goals and typical telescope configurations, are summarized in Table 1. Based on

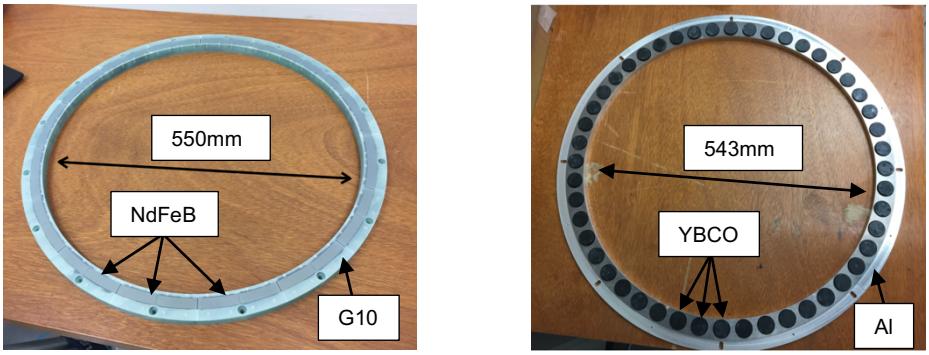

Figure 1. The left photograph shows a 32-segmented NdFeB permanent magnet ring with an inner diameter of 550mm, and the right photograph shows the ring-shaped superconductor consisting of 48 segmented cylinder YBCO bulks.

these requirements, we designed and manufactured an SMB system for a polarization modulator on SO. It consists of a permanent magnet ring and a ring-shaped high-temperature superconductor bulk, as shown in Figure 1. The limitation on the SMB diameter in prior experiments is < 460 mm, which is driven by the manufacturing limitations of the magnet ring for use at cryogenic temperatures. At room temperature, there are many examples of large continuous magnetic circuits with a diameter > 1 m for a magnetic resonance imaging (MRI) [8] and for Spring-8 [9]. However, at cryogenic temperatures, a dedicated design is required that considers thermal contraction and magnetic field variation. Therefore, we designed and manufactured a magnet ring with an inner diameter of 550 mm considering cryogenic properties, with the collaboration of Shin-Etsu Chemical Co., Ltd. It consists of 32 segmented NdFeB (N52) magnets and a G10 glass-epoxy holder. The width and height of the magnet are 15 mm to ensure sufficient magnetic field strength, which scales with the magnetized volume. The total mass of the ring magnet is 4.6 kg, and the inner and outer diameters are 550 mm and 620 mm, respectively. The gap between magnet segments is designed at 0.3 mm to consider for thermal contraction at around 50 K and assembly accuracy. The magnet and holder are glued by a Stycast 2850FT. To seal the magnet, a 1 mm thin cover with ventilation screw holes is installed on the surface of the magnet.

The superconductor ring consists of 48 segmented single-seeded YBCO bulks and an aluminum (A6061) holder. The YBCO bulks are supplied by CAN SUPERCONDUCTORS, s.r.o. Each bulk is cylindrical, and the diameter and height are 28 mm and 10 mm, respectively. The levitation force specification for these bulks at 77 K on the YBCO bulk surface is > 60N. The YBCO bulk is magnetized using a 20 mm × 20 mm NdFeB permanent magnet of ~ 0.5 Tesla magnetic field at the surface. The YBCO bulks and glued into the holder by Stycast 2850FT. The thickness of the holder is 8 mm, and the YBCO bulks are exposed above the holder's surface by 2 mm.

Table 1. Typical requirements for the polarization modulator in current and planned CMB ground experiments.

Inner/outer diameter	Rotation speed	Rotor/stator temperature	Heat dissipation	Total mass	Rotor position tolerance
$\Phi_{in} > 500$ mm $\Phi_{out} < 1000$ mm	2 Hz	$T_{rotor} < 60$ K $T_{stator} < 100$ K	< 1 W	40 kg	< 1 mm

2.2. Experimental setup

For the performance test of the developed SMB, we built an experimental setup in liquid nitrogen, as shown in Figure 2. We prepared a 1 m diameter stainless steel container with a glass fiber cloth and styrofoam for thermal insulation. A cryogenic hall sensor HGT-3020 from Lake Shore Cryogenics, Inc. is mounted on the surface of one of the YBCO bulks. The sensor was calibrated by the company

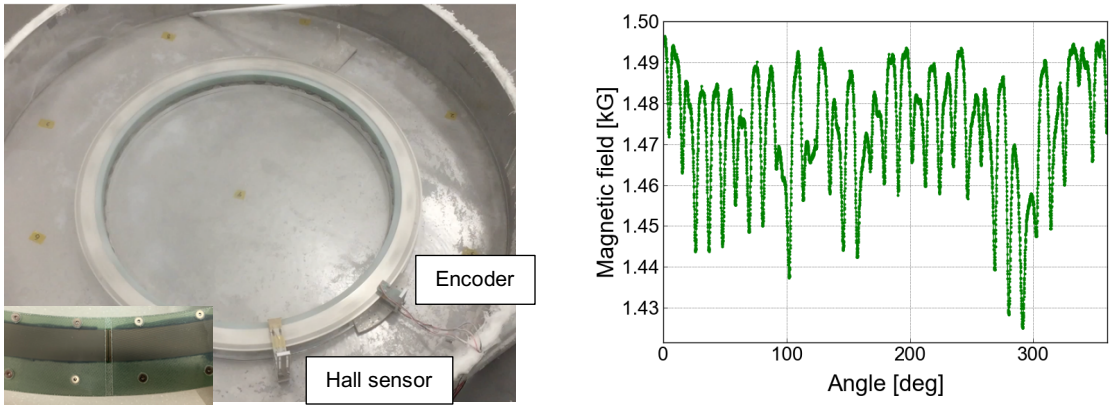

Figure 2. The left photograph shows the SMB performance test in liquid nitrogen. The right plot shows the magnetic field distribution vs. ring magnet angle, measured by a cryogenic hall sensor mounted on the surface of one of the YBCO bulks.

considering nonlinearity between the output voltage and the magnetic field, as well as temperature and angle effects. The zero field is calibrated within a magnetic shield, and the accuracy specification of the sensor is $\pm 1\%$. An optical encoder composed of an infrared LED and a silicon photodiode placed face to face is installed. An encoder disk with 360 slots on either side of an encoder disk with 360 slots, which is installed on top of the rotor magnet ring. The initial distance between the rotor magnet and the stator YBCO is 6 mm. We prepared a dedicated jig to establish the levitation height and the centering of the rotor magnet.

At room temperature, the YBCO stator and the rotor magnet with the dedicated jig are installed in the container. In addition, the hall sensor and the encoder with their own jig is mounted on the YBCO holder. Then, the liquid nitrogen is poured into the container. After field cooling, the dedicated jig is removed, and the rotor magnet levitates. In the spin-down and stiffness tests, the rotation and the vibration of the rotor were applied by hand.

3. Performance test

3.1. Magnetic field homogeneity

The main sources of SMB losses are hysteresis and eddy currents. The energy losses by hysteresis P_h and eddy current P_e can be described as

$$P_h \propto \frac{\Delta B^3}{J_c}, \qquad P_e \propto \Delta B^2 , \tag{1}$$

where ΔB is the magnetic field homogeneity of the rotor magnet and J_c is a critical current density of the YBCO bulks, which scales inversely with temperature. The magnetic field homogeneity is the key parameter that determines the SMB loss. We measured the magnetic field fluctuation using the cryogenic hall sensor as shown in the right plot of Figure 2. There are 32 spikes in the plot corresponding to the gap between magnet segments. The peak-to-peak homogeneity of the magnetic field is 4.8%, which is slightly better than that of the prior experiment [6].

3.2. Spin-down measurement

We conducted a spin-down test to measure power dissipation from the SMB [10,11]. The rotor is accelerated to ~1.2 Hz by hand. The maximum speed is limited by air resistance. Then the rotor decelerates due to magnetic and air friction. The rotation frequency during the spin down is shown in the left plot of Figure 3. The fit function is

$$a(t) = a_0 + 2\pi a_1 f(t), \tag{2}$$

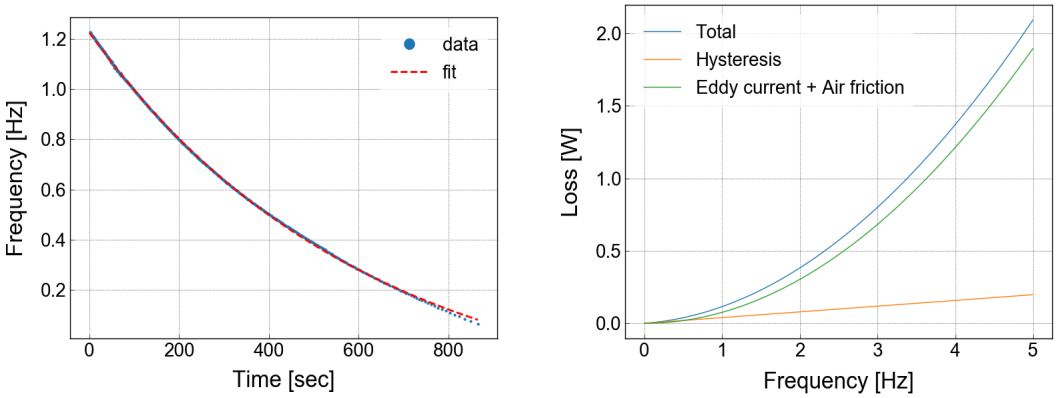

Figure 3. The left plot shows the SMB spin-down data. The blue dot shows the measured data and the dashed red line shows the fit line. The right plot shows the loss as a function of the rotation frequency. The blue, orange, green lines show the total loss, the hysteresis loss, and the eddy current + air friction losses, respectively.

$$f(t) = \frac{1}{2\pi a_1} e^{2\pi a_1 t} - \frac{a_0}{2\pi a_1}, \quad (3)$$

where *f(t)* is a rotation frequency, *a(t)* is a rotation deceleration and a_0, a_1 are deceleration terms due to hysteresis and eddy current + air friction, respectively. The heat dissipation *P* can be described as

$$P = I \times \tau, \; I = \frac{1}{2} m({R_{out}}^2 - {R_{in}}^2), \; \tau = a \times \omega = a \times 2\pi f \quad (4)$$

where *I* is the inertia of the rotor magnet, τ is the load torque on the rotor and *m* is the rotor mass. R_{out} and R_{in} represent the inner and outer radius of the rotor magnet, respectively. ω and *f* are the angular velocity and the rotation frequency of the rotor during continuous rotation, respectively. The total heat dissipation from the SMB is 0.39 W assuming 2 Hz continuous rotation, including due to air resistanc. This result satisfies the typical requirement of < 1.0 W. The estimated hysteresis loss is 0.08W, while the eddy current + air friction loss is 0.31 W. The right plot of Figure 3 shows the SMB losses for each continuous rotation speed.

3.3. Stiffness measurement

Another critical parameter to SMB performance is the bearing stiffness. We must trace rotor displacement due to gravity because it corresponds to HWP position in the polarization modulator. We modeled the stiffness as a spring constant, assuming the SMB to be a simple spring. The spring constant of the SMB increases in proportion to the gradient of the magnetic field, and thus this assumption is conservative. The levitating rotor vibrates according to its eigenfrequency [12]. The left plot of Figure 4 shows the magnetic field distribution when the rotor is hit multiple times, while the right plot shows the Fourier transform of the left plot. The first peak corresponds to the eigenfrequency of the SMB. The 2rd and 3rd peaks in the plot correspond to the 3rd and 5th harmonics because the SMB is assumed to be a spring with only one fixed end. The measured eigenfrequency f_0 is 24 Hz. The spring constant *k* and the rotor displacement due to gravity *x* can be calculated as

$$k = m\omega^2 = m(2\pi f_0)^2, \qquad x = \frac{mg}{k}, \quad (4)$$

where ω is angular frequency and *m* is the rotor mass. The calculated spring constant and the rotor displacement are 1.0×10^5 N/m and 0.46 mm, respectively. A typical requirement of the rotor displacement is < 1.0 mm, and therefore this test confirms that the developed SMB is sufficiently stiff for ground-based applications. Note that the rotor displacement due to the SMB stiffness is independent of alignment accuracy.

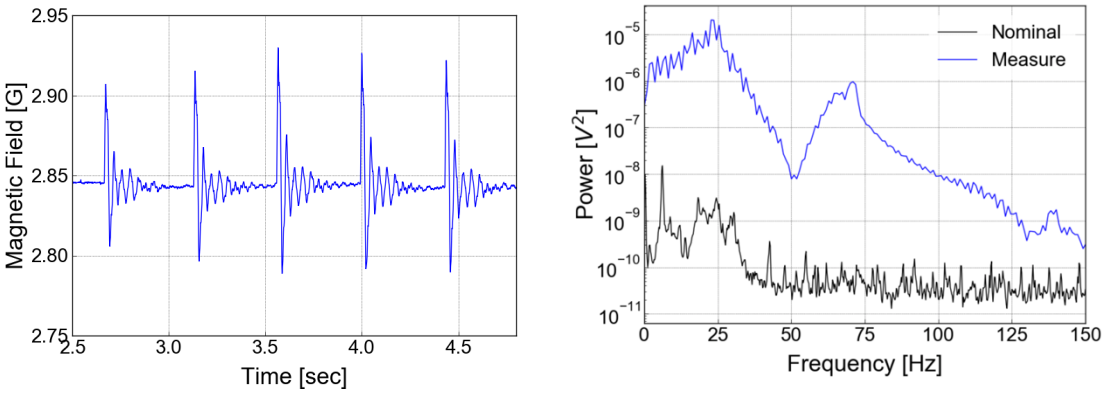

Figure 4. The left plot shows the magnetic field distribution when the ring magnet is struck. The right plot shows the Fourier transformed distribution of the left plot. The blue and black line shows the measured data with and without hitting.

4. Number of YBCO dependence

In order to test the dependence of rotor stiffness on YBCO configuration, the performance test was done with various numbers of YBCO bulks. The number of YBCO tiles were varied from 48 to 24 and 12 while keeping the gap between bulks equal, shown in Figure 5. We repeated the SMB performance test with the same procedure described in Section 3. The right plot of Figure 5 shows the magnetic field distribution for each YBCO configuration. The magnetic field strength and fluctuation increased when reducing the number of YBCO, which suggests a reduction in spring constant and hence levitation force.

We conducted the spin-down test and derived the SMB losses for each number of YBCO tiles, as shown in the left plot of Figure 6. The measured hysteresis loss increases in proportion to the cube of ΔB, as shown in Equation (1). As the eddy current loss, which depends on the square of ΔB, cannot be classified due to air friction. Because the air friction term depends on the convection state of nitrogen in each experiment, it is difficult to model and distinguish it from eddy currents. We performed the stiffness test for each number of YBCO tiles, as shown in the right plot of Figure 6. The measured eigenfrequency and the derived spring constant change in proportion to the number of YBCO tiles. The obtained parameters are summarized in Table 2.

These results are consistent with the levitation force model for the SMB. It is described as

$$F = \int_{\Omega_{SC}}^{0} (\boldsymbol{J} \times \boldsymbol{B})\, d\Omega_{SC}, \tag{5}$$

where F is the levitation force of the SMB, Ω_{SC} is the cross-section of the superconductor, $\boldsymbol{J}$ is the critical current density, and $\boldsymbol{B}$ is the magnetic field density [14]. Comparing the case of 48 and 24 tiles, the

Table 2. Measured and derived parameters from the performance test

Number of YBCO	48	24	12
|B|	1.47 kG	1.65 kG	1.69 kG
Δ B	0.09 kG	0.12 kG	0.13 kG
Total loss at 2 Hz	0.428 W	0.491 W	0.537 W
Hysteresis loss at 2 Hz	0.020 W	0.047 W	0.057 W
Eddy current + air friction loss at 2 Hz	0.402 W	0.459 W	0.490 W
Eigenfrequency	24 Hz	17 Hz	13 Hz
Spring constant	1.0×10^5 N/m	5.2×10^4 N/m	3.2×10^4 N/m
Rotor displacement	0.46 mm	0.88 mm	1.49 mm

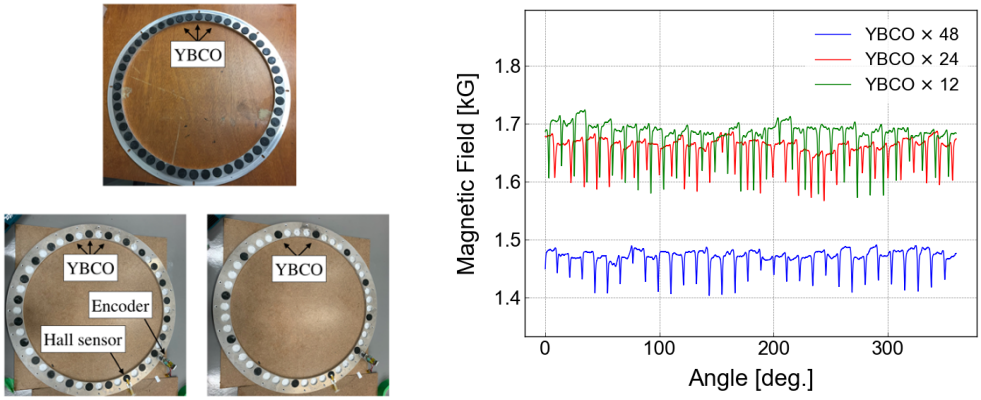

Figure 5. The left photograph shows the YBCO superconductor ring by changing the number of YBCO bulks. The right plot shows the magnetic field distribution for the ring magnet angle. The blue, red, and green lines show the number of YBCO as 48, 24, and 12, respectively.

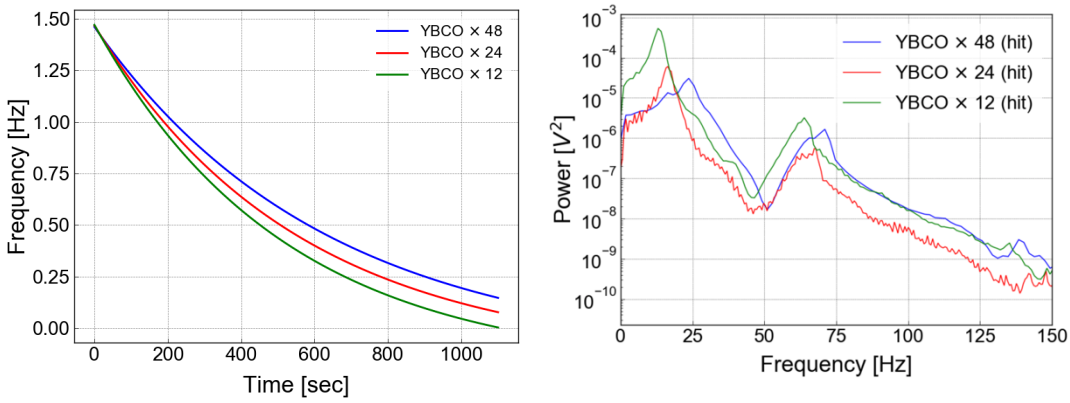

Figure 6. The left and right plot shows the spin-down distribution and the Fourier transformed distribution of the magnetic field, respectively, when hitting the rotor magnet for each number of YBCO tiles. The blue, red, and green lines show the number of YBCO as 48, 24, and 12, respectively.

levitation force is determined by the variation in both the magnetic field density and the volume of the YBCO bulks. On the other hand, comparing the case of 24 and 12 tiles, the effect from the magnetic field density cannot be ignored considering the accuracy of the hall sensor. However, it is determined almost entirely by the variation of the YBCO volume, as the displacement of the rotor position corresponding to the magnetic field density is almost saturated due to the reduced magnetic field gradient.

5. Conclusion

We designed and manufactured the world's largest SMB used in a polarization modulator for next-generation ground-based CMB polarization experiments. We conducted mechanical and thermal performance tests in liquid nitrogen.

The peak-to-peak homogeneity of the magnetic field of the rotor magnet is measured to be 4.8 %, which is a slightly better result than that of prior experiments. The heat dissipation due to the SMB is derived from spin-down testing. The total loss at 2 Hz continuous rotation is 0.4 W, which satisfies the typical requirement of < 1.0 W. The bearing stiffness is evaluated as a spring constant. It is derived from the rotor eigenfrequency, which is measured by hitting the rotor magnet. The obtained spring constant is 1.0×10^5 N/m, and the corresponding rotor position displacement due to gravity is 0.46 mm, assuming a simple spring model. The typical requirement on the rotor position tolerance is < 1.0 mm, and therefore the bearing is confirmed to be sufficiently stiff.

Furthermore, we carried out a performance test by changing the number of YBCO bulks, and we observed its impact on both loss and stiffness. These results are consistent with the SMB model, which predicts that the levitation height is proportional to the magnetic field density and the superconductor volume.

There is much room to reduce the SMB loss and increase its stiffness. For example, the magnetic field homogeneity can be improved by introducing a dedicated uniform magnetic ring combining permanent magnets and magnetic yokes, and the levitation force can be increased by using a continuous superconductor ring instead of cylinder-shaped bulks. However, we confirmed that the tested SMB performance satisfies typical experimental requirements. Therefore, the developed SMB for the polarization modulator is functionally optimized in terms of performance, cost, lead time, and manufacturing complexity.

Acknowledgements

This work was supported by MEXT KAKENHI Grant Numbers, JP19H00674, 17H06134, 16K21744 JP17K14272, and JP19K14732. This work was also supported by JSPS Core-to-Core Program, Advanced Research Networks and World Premier International Research Center Initiative (WPI) MEXT Japan, and JSPS Leading Initiative for Excellent Young Researchers (LEADER). The work at LBNL is supported in part by the U.S. Department of Energy, Office of Science, Office of High Energy Physics, under contract No. DE-AC02-05CH11231. The authors would like to thank Shin-Etsu Chemical Co., Ltd. for the cooperation of the manufacturing of the ring magnet. We would like to thank Editage (www.editage.com) and American Manuscript Editors (www.americanmanuscripteditors.com) for English language editing.

References

[1] Sato K 1981 First-order phase transition of a vacuum and the expansion of the Universe Monthly Notices of Royal Astronomical Society 195 46
[2] Guth Alan H 1981 The Inflationary Universe: A Possible Solution to the Horizon and Flatness Problems *Phys. Rev.* D **23** 347
[3] Kusaka A *et al*. 2014 Modulation of cosmic microwave background polarization with a warm rapidly rotating half-wave plate on the Atacama B-Mode Search instrument *Review of Scientific Instruments* **85** 024501
[4] Hull J 2000 TOPICAL REVIEW: Superconducting bearings *Superconductor Science and Technology* **13** 2 1-15
[5] Klein J *et al*. 2011 A cryogenic half-wave plate polarimeter using a superconducting magnetic bearing *Proceedings of the SPIE* **8150** 815004
[6] Hill C. A. *et al*. 2016 Design and development of an ambient-temperature continuously-rotating achromatic half-wave plate for CMB polarization modulation on the POLARBEAR-2 experiment *Proceedings of SPIE* **9914** 99142U
[7] Galitzki N *et al*. 2018 The Simons Observatory: instrument overview *Proceedings of SPIE* **10708** 1070804
[8] Cosmus T.C. and Parizh M 2011 Advances in whole-body MRI magnets *IEEE Trans AppIed Superconductivity* **21** 3.
[9] Tanaka H 2016 Spring-8 Upgrade Project *7th Int. Particle Accelerator Conf. (IPAC2016)*
[10] Sakurai Y, Matsumura T, Kataza H, Utsunomiya S and Yamamoto R 2017 Estimation of the heat dissipation and the rotor temperature of superconducting magnetic bearing below 10 K *IEEE Transactions on Applied Superconductivity* **27** 4
[11] Sakurai Y *et al*. 2018 Design and thermal characteristics of a 400mm diameter levitating rotor in a superconducting magnetic bearing operating below at 10K for a CMB polarization experiment *IEEE Transaction on Applied Superconductivity* **28** 4 1-4
[12] Sakurai Y, Matsumura T, Sugai H, Katayama N, Ohsaki H, Terao Y, Terachi Y, Kataza H, Utsunomiya S and Yamamoto R 2017 Vibrational characteristics of a superconducting magnetic bearing employed for a prototype polarization modulator *Journal of Physics: Conference Series* **871** 012091
[13] Sakurai Y, Matsumura T, Katayama N, Iida T, Komatsu K, Sugai H, Ohsaki H, Terao Y, Hirota Y and Enokida H 2019 Development of a contact-less cryogenic rotation mechanism employed for a polarization modulator unit in cosmic microwave background polarization experiments. *Journal of Physics: Conference Series* **1293** 012083
[14] Quéval L, Liu K, Yang W, Zermeño V.M.R. and Ma G 2018 Superconducting magnetic bearings simulation using an H-formulation finite element model *Superconductor Science and Technology* **31** 8